A Look at a Novel Antenna Design

Prof. Dr. Ing.-habil. Ulrich L. Rohde
Department of Electrical Engineering
School of Computation, Information and Technology
Technical University of Munich

Prof. James K. Breakall
Department of Electrical Engineering
School of Electrical Engineering and Computer Science
Penn State University
University Park, PA 16802

April 11, 2023

This discussion is triggered in part by the book [1], and the need to have small antennas with good front to back ratios. Needed for this are modern mathematical tools as well as test equipment.

As an example of mathematical tools, Hallén wrote his famous integral equation to give an exact treatment of antenna current wave reflection at the end of a tube shaped cylindrical antenna in 1956, but his first work on this subject [2] probably goes back to 1938. This equation enabled him to show that on a thin wire the current distribution is approximately sinusoidal and propagates with nearly the speed of light. For this treatment that is an important contribution.

We will learn here that by optimizing the effective length of a rod antenna, it will become directional and will have a radiation pattern that provides gain. Any antenna has a physical dimension, and the most relevant one is the antenna height. For a ground mounted vertical antenna, the mirror image in the ground is also considered, and the total length is called the effective length. In this discussion only the magnitude of l_{eff} is of interest. The definition of "effective length" is going to be the key point and its value can generate some "interesting effects".

In general, following the common tradition we assume all ideal conditions for a better understanding of the topic!

Now let us get started:

Antennas are key elements for communication, both for receive and transmit and there is a certain fascination with their design,

It all started with the Hertzian dipole as illustrated in Fig. 1(a) and its understanding and mathematical treatment [3].

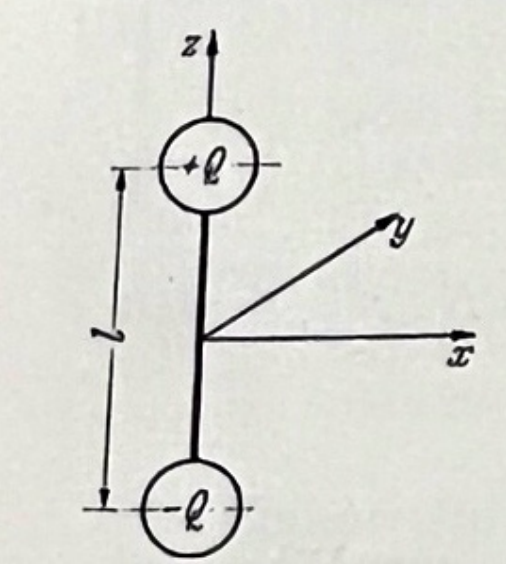

Fig 1. (a) Electrical dipole, charges +Q and -Q are changing periodically and harmonically as a function of t and with period T (sinusoidal). Source: [3].

It is assumed that the charges change periodically producing a current

$$i = -\frac{dQ}{dt} = -\frac{1}{l}\frac{df(t)}{dt} = +\frac{2\pi Q_0}{T}\sin\left(\frac{2\pi t}{T}\right) += +2\pi\nu Q_0 \sin(2\pi\nu t),$$

where

$$f(t) = Q_0 l\ \cos\left(\frac{2\pi t}{T}\right) = Q_0 l \cos(\omega t).$$

Again, here mostly the magnitude of $l_{\text{eff}} = l$ is of interest.

Now let's look at the real-life situation. An electric field (E_i) multiplied with the effective length of the antenna (l_{eff}) generates an EMF (electromotive force).

We also notice that the antenna wire is not straight but has a specific shape, this will be the topic of this discussion. The effective length of an antenna multiplied with the electrical field E_i results in an EMF V_0, seen in Fig. 1(b).

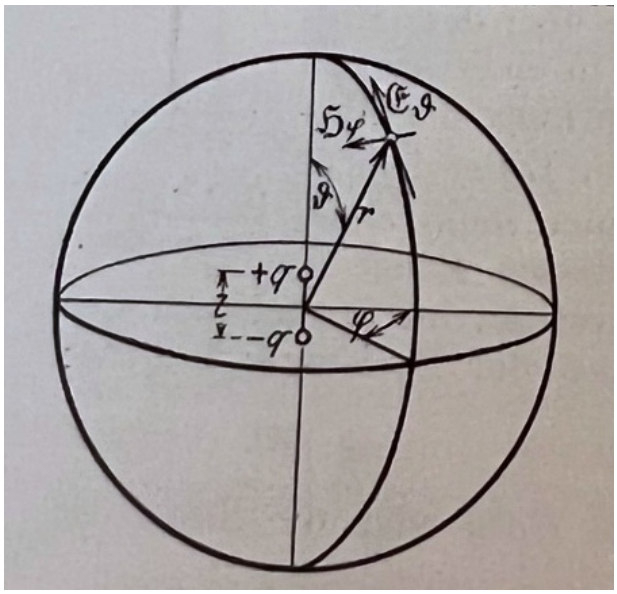

Fig. 1(b): Polar Co-ordinates around the Dipole, see the charges +*q* and –*q*. Source: [3].

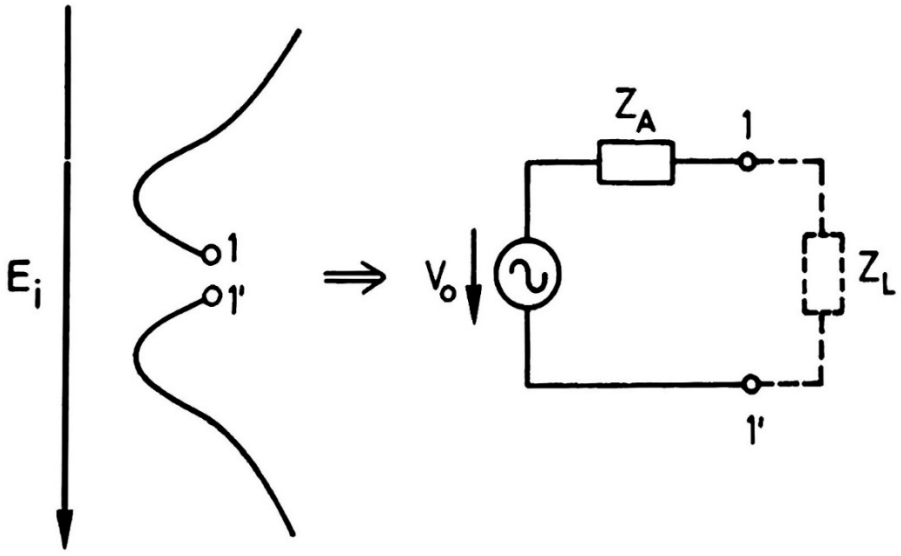

Fig. 2: The equivalent circuit of an antenna exposed to an electric field E_i. Source: [3].

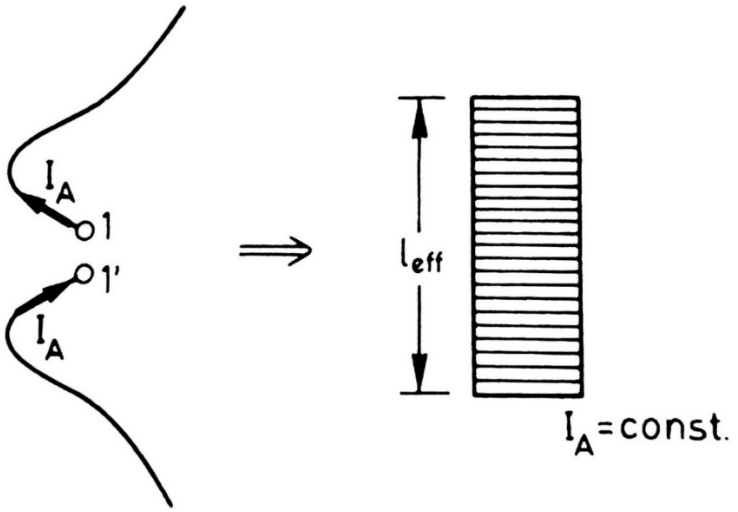

Fig. 3. Showing the effective length l_{eff}. Source: [3].

The following derivation is based in part on [1].

The following equations show the vector components of the electrical and magnetic fields relative to the isotropic antenna:

$$\mathfrak{E}\text{x} = \frac{3xz}{r^5}f + \frac{3xz}{cr^4}f' + \frac{xz}{c^2r^3}f'' = \left[\frac{3}{r^3}f + \frac{3}{cr^2}f' + \frac{1}{c^2r}f''\right]\cos\varphi\cos\vartheta\sin\vartheta,$$

$$\mathfrak{E}\text{y} = \frac{3yz}{r^5}f + \frac{3yz}{cr^4}f' + \frac{yz}{c^2r^3}f'' = \left[\frac{3}{r^3}f + \frac{3}{cr^2}f' + \frac{1}{c^2\gamma}f''\right]\sin\varphi\cos\vartheta\sin\vartheta,$$

$$\mathfrak{H}\text{z} = \frac{3z^2 - r^2}{r^5}f + \frac{3z^2 - r^2}{cr^4}f' + \frac{z^2 - v^2}{c^2r^3}f'',$$

$$= -\left[\frac{f}{r^3} + \frac{1}{cr^2}f' + \frac{1}{c^2r}f''\right] + \left[\frac{3}{r^3}f + \frac{3}{cr^2}f' + \frac{1}{c^2r}f''\right]\cos^2\vartheta\,,$$

$$\mathfrak{H}\text{x} = \frac{y}{cr^3}f' - \frac{y}{c^2r^2}f'' = -\frac{1}{c}\left[\frac{f'}{v^2} + \frac{1}{cr}f''\right]\sin\varphi\sin\vartheta\,,$$

$$\mathfrak{H}\text{y} = \frac{x}{cr^3}f' + \frac{x}{c^2r^2}f'' = +\frac{1}{c}\left[\frac{f'}{v^2} + \frac{1}{cr}f''\right]\cos\varphi\sin\vartheta\,,$$

$$\mathfrak{H}\text{z} = 0$$

$$\mathfrak{E}_\vartheta = -\left[\frac{f}{r^3} + \frac{1}{cv^2}f' + \frac{1}{c^2r}f''\right]\sin\vartheta\,,$$

$$\mathfrak{E}_r = 2\left[\frac{f}{r^3} + \frac{f'}{cr^2}\right]\cos\vartheta\,,$$

$$\mathfrak{E}_\varrho = \sqrt{\mathfrak{E}_x^2 + \mathfrak{E}_y^2} = \frac{z\varrho}{r^3}\left[\frac{3f}{v^2} + \frac{3f'}{cv} + \frac{f''}{c^2}\right],$$

$$\mathfrak{E}_z = \frac{2}{v^2}\left[\frac{f}{r} + \frac{f'}{c}\right] - \frac{\varrho^2}{r^3}\left[\frac{3f}{v^2} + \frac{3f'}{cv} + \frac{1}{c^2}f''\right],$$
$$\mathfrak{H}_\varphi = -\frac{\varrho}{r^2}\left[\frac{f'}{cv} + \frac{1}{c}f''\right],$$

where $\varrho = \sqrt{x^2 + y^2}$.

Here are the function *f* and its derivatives referred to above:

$$f(t) = \frac{I_0 l}{\omega}\cos\left(\omega\left(t - \frac{r}{c}\right)\right) = Q_0 l \cos\left(\omega\left(t - \frac{r}{c}\right)\right).$$
$$f'(t) = -I_0 l \sin\left(\omega\left(t - \frac{r}{c}\right)\right) = -Q_0 l\omega \sin\left(\omega\left(t - \frac{r}{c}\right)\right),$$
$$f''(t) = -I_0 l\omega \cos\left(\omega\left(t - \frac{r}{c}\right)\right) = -Q_0 l\omega^2 \cos\left(\omega\left(t - \frac{r}{c}\right)\right).$$

The part (*t* - *r/c*), where *t* is time, *r* is the length of the vector and *c* the speed of light, indicates that there is a delay of the electromagnetic wave which is delayed at the distance '*r*' at the time '*t*' so the value of the function cannot be achieved at the time '*t*', the delay is *r/c*, called retardation.

For the far field the results are:

$$\left.\begin{aligned}
&\mathfrak{E}_x = \tfrac{1}{c^2 r} f'' \cos\varphi \cos\vartheta \sin\vartheta\,, \quad \mathfrak{H}_x = -\tfrac{1}{c^2 r} f'' \sin\varphi \sin\vartheta,\\
&\mathfrak{E}_y = \frac{1}{c^2 r} f'' \sin\varphi \cos\vartheta \sin\vartheta, \quad \mathfrak{H}_y = +\frac{1}{c^2 r} f'' \cos\varphi \sin\vartheta\\
&\mathfrak{E}_z = -\frac{1}{c^2 r} f'' \sin^2\vartheta, \qquad\qquad \mathfrak{H}_z = 0
\end{aligned}\right\}$$
$$\mathfrak{H}_\varphi = -\tfrac{1}{c^2 r} f'' \sin\vartheta,$$
$$\mathfrak{E}_r = 0,$$
$$\mathfrak{H}_\varphi = -\frac{1}{c^2 r} f'' \sin\vartheta$$
$$\mathfrak{E}_\varrho = \tfrac{2\varrho}{c^2 r^3} f'' = \tfrac{1}{c^2 r} f'' \cos\vartheta \sin\vartheta,$$
$$\mathfrak{E}_z = -\tfrac{\varrho^2}{r^3 c^2} f'' = -\tfrac{1}{c^2 r} f'' \sin^2\vartheta,$$
$$\mathfrak{H}_\varphi = -\tfrac{1}{c^2 r} f'' \sin\vartheta,$$

$$\left.\begin{aligned}
\mathfrak{E}_\partial &= \frac{2\pi I_0 l}{cr\lambda}\sin\vartheta\cos\left(\omega\left(t-\frac{r}{c}\right)\right) = \frac{4\pi^2 Q_0 l}{\lambda^2 r}\sin\vartheta\cos\bar{\omega},\\
\mathfrak{E}_r &= 0,\\
\mathfrak{H}_\varphi &= -\frac{2\pi I_0 l}{cr\lambda}\sin\vartheta\cos\left(\omega\left(t-\frac{r}{c}\right)\right) = -\frac{4\pi^2 Q_0 l}{\lambda^2 r}\sin\vartheta\cos\bar{\omega},\\
\mathfrak{E}_\varrho &= -\frac{2\pi I_0 l}{cr\lambda}\sin\vartheta\cos\vartheta\cos\left(\omega\left(t-\frac{r}{c}\right)\right) = -\frac{4\pi^2 Q_0 l}{\lambda^2 r}\sin\vartheta\cos\vartheta\cos\bar{\omega},\\
\mathfrak{E}_z &= \frac{2\pi I_0 l}{cr\lambda}\sin^2\vartheta\cos\left(\omega\left(t-\frac{r}{c}\right)\right) = \frac{4\pi^2 Q_0 l}{\lambda^2 r}\sin^2\vartheta\cos\bar{\omega},\\
\mathfrak{H}_\varphi &= -\frac{2\pi I_0 l}{6r\lambda}\sin\vartheta\cos\left(\omega\left(t-\frac{r}{c}\right)\right) = -\frac{4\pi^2 Q_0 l}{\lambda^2 r}\sin\vartheta\cos\bar{\omega}.
\end{aligned}\right\}$$

As a result of this we can calculate the field at various regions:

$$\mathfrak{E}_z = \frac{4\pi^2}{\lambda^2}\frac{T_0 l}{c}\Big[\underbrace{\frac{2-3\sin^2\vartheta}{a^3}\cos\left(\omega\left(t-\frac{a\lambda}{2\pi c}\right)\right)}_{\text{Near flield}} + \underbrace{\frac{3\sin^2\theta-2}{a^2}\sin\left(\omega\left(t-\frac{a\lambda}{2\pi c}\right)\right)}_{\text{Middle field}} + \underbrace{\frac{\sin^2\vartheta}{a}\cos\left(\omega\left(t-\frac{a\lambda}{2\pi c}\right)\right)}_{\text{Far field}},$$

with $a = 2\pi r/\lambda$.

The total radiation is

$$N_{S_T} = \frac{I_0^2\omega^2 l^2}{4\pi c^3}\int_0^{2\pi}\int_0^{\pi}\int_0^{T}\cos^2\frac{2\pi}{T}\left(t-\frac{r}{c}\right)d\varphi\,\sin^3\vartheta d\vartheta dt\,,$$

$$N_{S_T} = \frac{I_0^2\omega^2 l^2 T}{3c^3} = \frac{4\pi^2 I_0^2}{3c}\left(\frac{l}{\lambda}\right)^2 T = \frac{16\pi^4 l^2 Q_0^2}{3\lambda^3}.$$

T: time period

The energy radiated is

$$N_S = \frac{4\pi^2 I_0^2}{3c}\left(\frac{l}{\lambda}\right)^2 = \frac{8\pi^2 I_{\text{ett}}^2}{3c}\left(\frac{l}{\lambda}\right)^2 = \frac{16\pi^4 l^2 Q_0^2 c}{3\lambda^4}.$$

Expressed I_{eff} in Ampere we get

$$N_S = 80\pi^2\left(\frac{l}{\lambda}\right)^2 I_{\text{eff}}^2 \text{ W}$$

or the Radiation resistance is

$$R_S = 80\pi^2 \left(\frac{l}{\lambda}\right)^2 \text{Ohm.}$$

The resulting radiation pattern as a function of time is shown in Fig. 4.

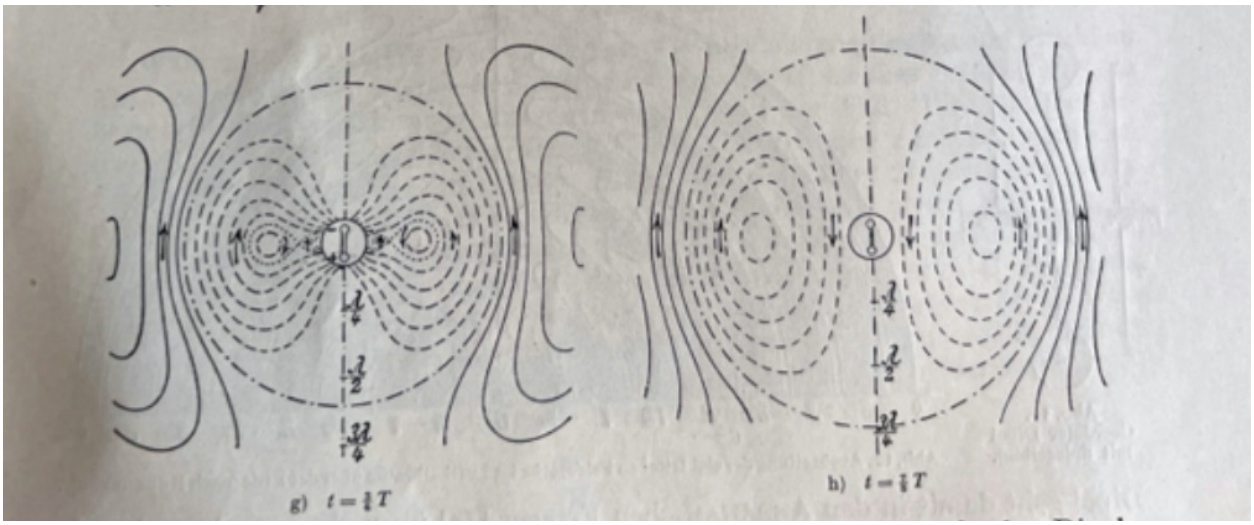

Fig. 4: Radiation pattern with reference to *T*. Source: [3].

Important: l is not the mechanical length but the electrical length, $l_{\text{eff}} \sim l/1.56$,

$$R_S = 80\pi^2 \left(\frac{l\ x\ 0.64}{\lambda}\right)^2 \text{Ohm} = 36.6.$$

Typically a factor of 2 is used, instead of 1.56, depending upon the definition of the length (mirror image in the ground). If the actual antenna at resonance due to the end effect is slightly inductive, it typically will be cut short and the error at the feeding point (imaginary part) will be compensated by a suitable matching network. The exact reason for the 0.64 correction factor is that the voltages and currents are sinusoidal only when the wire is very thin.

Fig. 5 presents a plot that shows the radiation resistance as a function of the length to wavelength ratio.

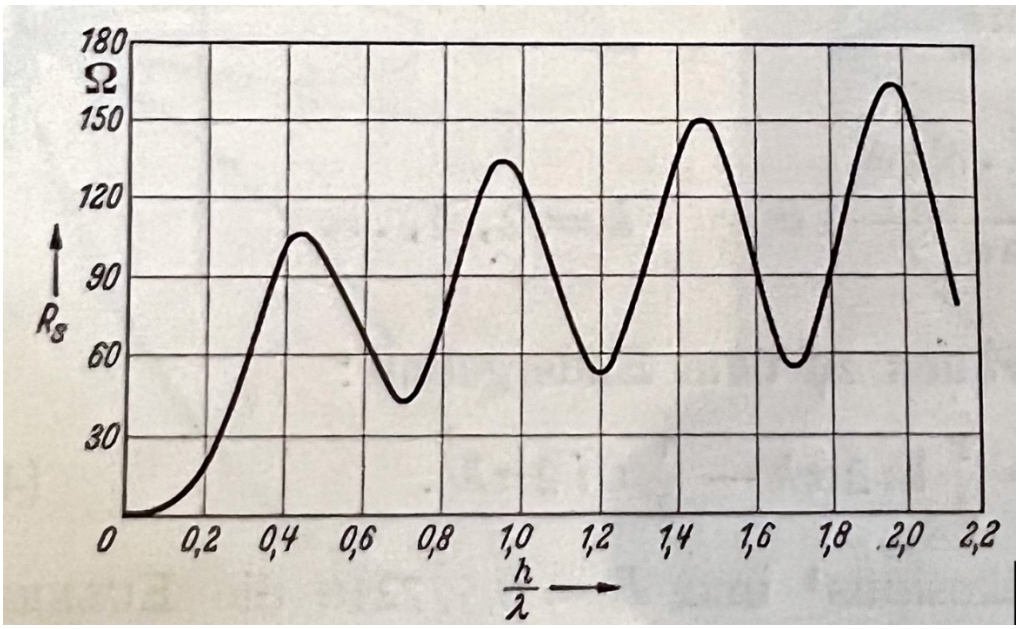

Fig. 5: Plot showing the radiation resistance as a function of the length to wavelength ratio. Source: [3].

If the radiating rod is curved as shown in Fig. 6, an approximation as shown below can be used to calculate the electrical field.

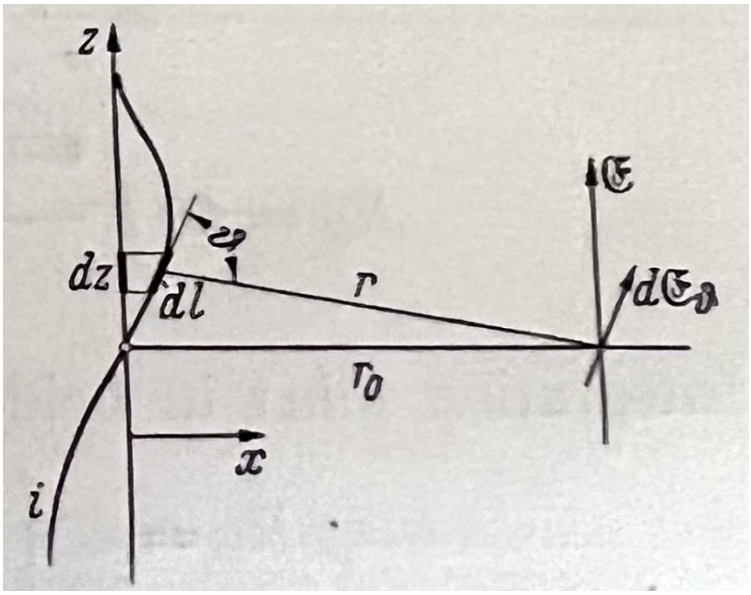

Fig 6: Approximate electrical field calculation for a curved radiating rod. Source: [3].

Fig. 7 (a)-(f) show the radiation patterns/curves as a function of varying time ωt.

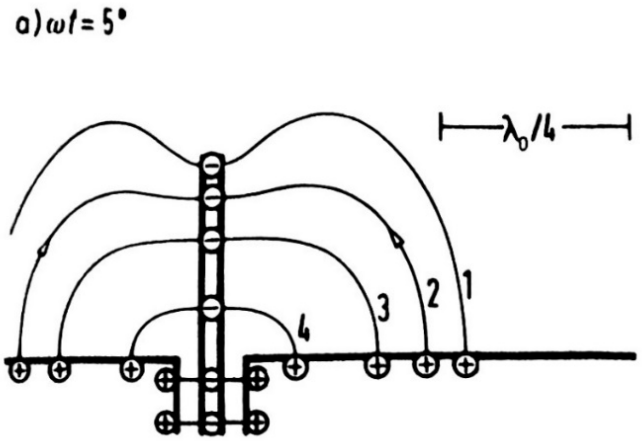

Fig. 7 (a): Radiation patterns as a function of different ωt (ωt=5° of 360°). Source: [3].

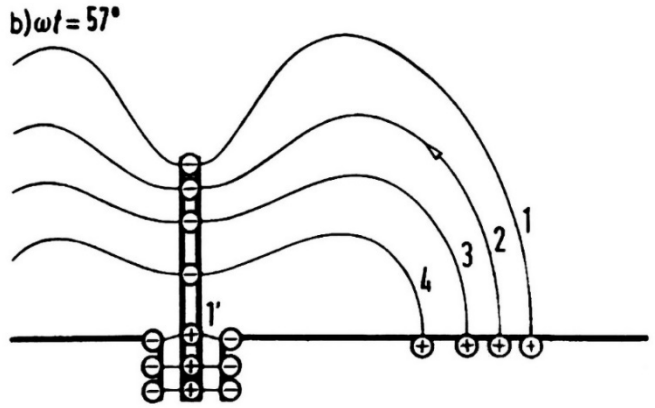

Fig. 7 (b): Radiation patterns as a function of different ωt (ωt=57°). Source: [3].

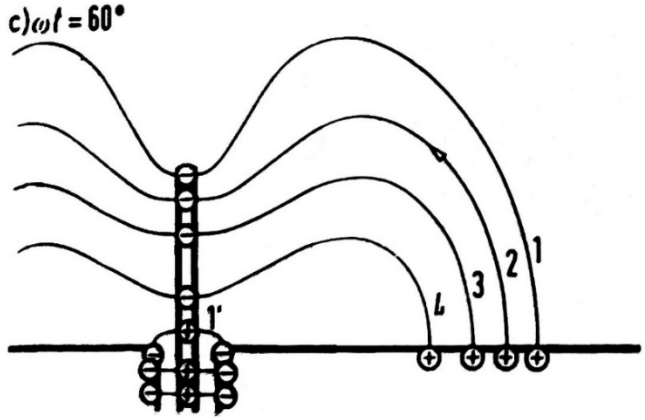

Fig. 7 (c): Radiation patterns as a function of different ωt (ωt=60°). Source: [3].

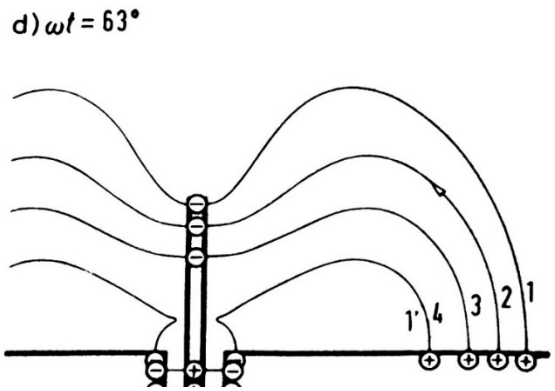

Fig. 7 (d): Radiation patterns as a function of different *ω*t (*ω*t=63°). Source: [3].

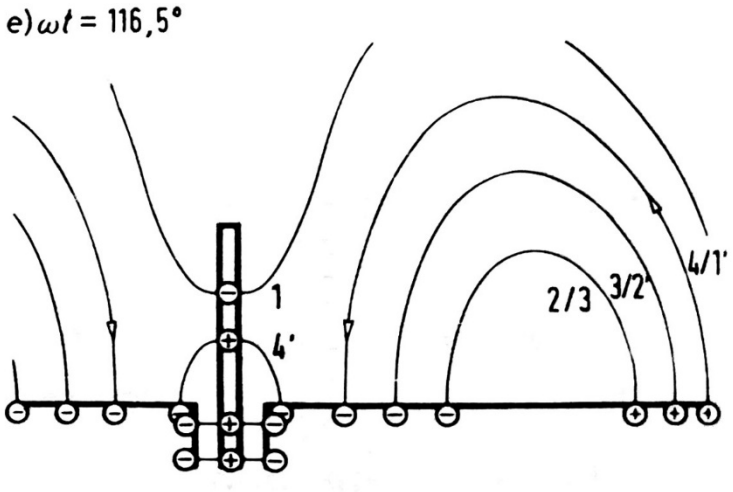

Fig. 7(e): Radiation patterns as a function of different *ω*t (*ω*t=116.5°). Source: [3].

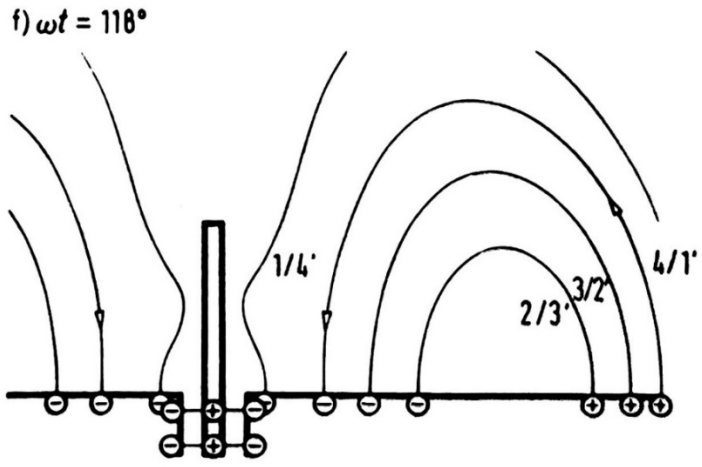

Fig. 7 (f): Radiation patterns as a function of different *ωt* (*ωt* = 118°). Source: [3].

The example shown in Fig. 7 (a)-(f), is a vertical rod antenna, as we all know. There are circumstances where the antenna is not straight but curved. An early example is a trailing antenna from an airplane [2].

As an example we will use the curved shape antenna shown in Fig. 8. It is interesting to know that the end effect of the antenna, as described by the Hallén's integral equation is equivalent to the end effect radiation in microstrips. This type of antenna is called a thin curvilinear monopole.

This assumes that the ratio (l/d) is smaller than 0.01.

The reason why the curved antenna is of interest is to make improvement to the military Manpack with the tilted antenna as shown in Fig. 8. If the antenna could be optimized in such a way that it shows gain, the effect of the building on the left side would be compensated for.

Fig. 8: Military Manpack with a straight whip antenna.

An antenna can also be described as an open-ended transmission line where the open end has the highest voltage and the other side has the highest current. To be specific, this transmission line is lossy, so the hyperbolic tension function is applicable. This also means compared to a parallel

tuned circuit, the antenna radiates at odd multiples (like 3, 5, 7…) of the fundamental frequency. The next relevant question is the input impedance. This can be determined from the following approximation equations [4] [8]-[10].

Input impedance $Z_{in} = (Z_a^2)/R_s$ (where R_s is the radiation resistance) with

$$Z_a = \sqrt{L_a/C_a},$$

where 'l' is the antenna length in meters and, 'd' is the wire diameter in meters.

As an example of a 4 MHz, 40 m long dipole (20 m each side) with 2 mm thickness would be

$$L_a = \left(\frac{l\mu_0}{2\pi}\ln\frac{4r}{D}\right) = 10\text{x}10^{-7}$$

$$C = \frac{20\text{ pF}}{\text{m}}, \qquad \text{so } C_a = 20x20 = 400\text{ pF}$$

$$Z_a = \sqrt{10\text{x}10^{-7}/400\text{x}10^{-12}} = 50\ \Omega$$

Let us assume a quarter wave antenna, with a radiation resistance of R_s of 36.6 Ω,

Input impedance $Z_{in} = (50)^2/36.6 = 68$, Z_a is an approximation.

The exact solution is obviously [9]

$$Z_{11} = 30\int_0^{j2\pi n}\frac{1-e^{-w}}{w}dw.$$

The integral Z_{11} is an exponential integral with imaginary argument.

In our case $y = 2\pi n$. This integral can be expressed in terms of the sine and cosine integrals.

The input-impedance is

$$Z_{11} = R_{11} + jX_{11} = 30[\text{Cin}(2\pi n) + j\,\text{Si}(2\pi n)],$$
$$Z_{11} = 30[0.577 + \ln(2\pi n) - \text{Ci}(2\pi n) + j\text{Si}(2\pi n)].$$

For a thin linear antenna of half a wavelength (S. A. Schelkunoff, Applied Mathematics for Engineers and Scientists, Van Nostrand, New York, 1948. p377) it is found

$$Z_{11} = j30\int_0^l\left(\frac{e^{-j\beta z}}{z} + \frac{e^{-j\beta(l-z)}}{l-z}\right)\sin\beta z\,dz.$$

Applying de Moivre's theorem to $\sin\beta z$, gives

$$Z_{11} = -15\int_0^l\left[\frac{e^{-j2\beta z}-1}{z} - \frac{e^{-j\beta L}\left(e^{j2\beta z}-1\right)}{l-z}\right]dz.$$

For $l = n\lambda/2$ where $n = 1,3,5, \ldots, e^{-j\beta l} = e^{-j\pi n} = -1$, so that (38) becomes

$$Z_{11} = -15\int_0^l \left(\frac{e^{-j2\beta z}-1}{z} + \frac{e^{j2\beta z}-1}{l-z}\right)dz$$

$$Z_{11} = 15\int_0^l \frac{1-e^{-j2\beta z}}{z}dz + 15\int_0^l \frac{1-e^{j2\beta z}}{l-z}dz$$

$$-15\int_{2\pi n}^0 \frac{1-e^{j(2\pi n - v)}}{v}dv = 15\int_0^{2\pi n}\frac{1-e^{-jv}}{v}dv$$

Equations (41) and (42) are definite integrals of identical form. Since their limits are the same, they are equal. Therefore, (40) becomes

$$Z_{11} = 30\int_0^{2\pi n}\frac{1-e^{-ju}}{u}du.$$

If we now set $w = ju$, (43) transforms to

$$Z_{11} = 30\int_0^{j2\pi n}\frac{1-e^{-w}}{w}dw$$

The integral in (44) is an exponential integral with imaginary argument.

This integral can be expressed in terms of the sine and cosine integrals

Hence, the input-impedance is

$$Z_{11} = R_{11} + jX_{11} = 30[\mathrm{Cin}(2\pi n) + \mathrm{jSi}(2\pi n)],$$
$$Z_{11} = 30[0.577 + \ln(2\pi n) - \mathrm{Ci}(2\pi n) + j\mathrm{Si}(2\pi n)].$$

The more general situation, where the antenna length l is not restricted at an odd number of $\lambda/2$, has also been treated. The antenna is center-fed, and the current distribution is assumed to be sinusoidal.

The input impedance for this case is

$$R_{11} = 30\left[\left(1-\cot^2\frac{\beta l}{2}\right)\mathrm{Cin}\,2\beta l + 4\cot^2\frac{\beta l}{2}\mathrm{Cin}\,\beta l + 2\cot\frac{\beta l}{2}\,(\mathrm{si}\,2\beta l - 2s\beta l)\right].$$

The above discussion of this section applies to balanced centered antennas. For a thin linear stub antenna of height 'l' perpendicular to an infinite, perfectly conducting ground, the self-impedance is half of that for the corresponding balanced type. The general formula for input resistance can be converted for a stub antenna above a ground plane by changing the factor 30 to 15 and making the

substitution $l = 21$. The formulas can be converted for a stub antenna with ground plane where the antenna is an odd number n of $\lambda/4$ long by changing the factor 30 to 15. In this case we get

$$Z_{11}=36.6 \text{ Ohm} + j\ 21 \text{ Ohm}$$

Assuming this antenna which should resonate at about 4 MHz, we can determine the combination of radiation losses and other losses. A FoM (figure of Merit) is the standing wave ratio of 2.6, and the actual 3dB bandwidth will be about 200 kHz. This means that the operating Q of the antenna is 20. These are not common losses, but are radiation losses [5].

Derivation:

The magnitude of the reflection coefficient rho is defined as

$$\rho(f) := \left(\left|\frac{Z(f) - R}{Z(f) + R}\right|\right)$$

If Z_{in} = (50+j50), half power (-3 dB) or (50-j50), other side of the 3 dB point,

Then the flection coefficient is at the bandwidth edges are

$$\rho\text{L} := \rho(\text{ Flow}) \qquad \rho\text{L} = 0.447,$$
$$\rho\text{H} := \rho(\text{ Fhigh }) \quad \rho\text{H} = 0.447.$$

Now find the VSWR versus frequency: $\text{VSWR(f)} := \frac{1+\rho(\text{f})}{1-\rho(\text{f})}$ and VSWR at the bandwidth edges:

$$\text{VSWR}(\text{ Flow }) = 2.618$$
$$\text{VSWR}(\text{ Fhigh }) = 2.618$$

If the bandwidth is much smaller, then there are some inductors or capacitors or a combination of (traps), inductors or capacitors, which make the antenna electrically longer at the expense of bandwidth.

Compared to the tube amplifiers modern transistorized amplifiers cannot handle a larger than 1.5 VSWR and reduce drastically the output power. While the tube amplifiers had a Collins or Low Pass filter at the output and could tune out mismatch the , the solid state amplifier needs to be held and resorts to an additional “line flattening circuit that most of the time can handle an VSWR of 3 and protects the output stage

Landstorfer [3] notes that curvilinear antennas of general shape suffer from the fact that experimental investigations as well as numerical analysis are restricted to a limited number of antennas with arbitrary shapes. It is not possible to show all the possibilities of curvilinear wire antennas as a whole. The first mention of a quasi curvilinear antenna was found in [2]. Here an antenna was dragged by an airplane. Let’s assume that it had the curve shown in Fig. 9 (a) and (b) [4].

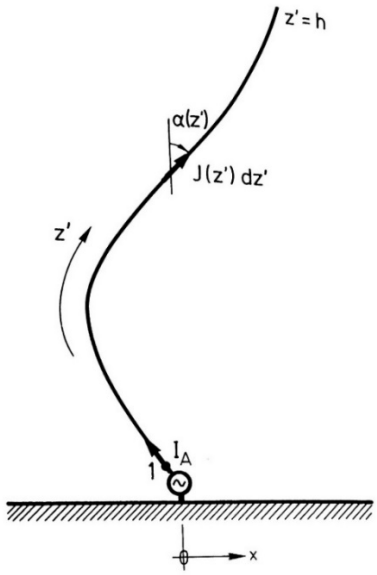

Fig. 9 (a): Curved antenna. Source: [3].

This curved antenna can be split in different sections (from 1, 2, 3, 4…. to n).

The following is a method to breakdown the antenna into small, straight, pieces.

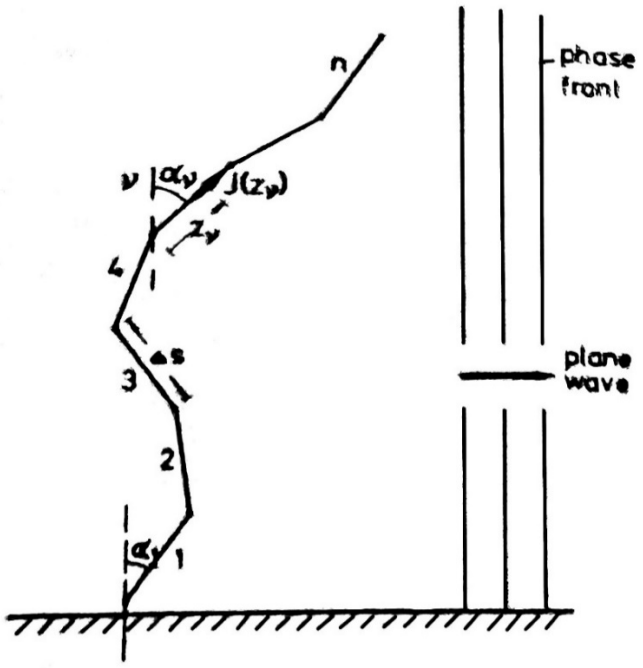

Fig. 9(b): Curved antenna split in numerous sections for analysis. Source: [3].

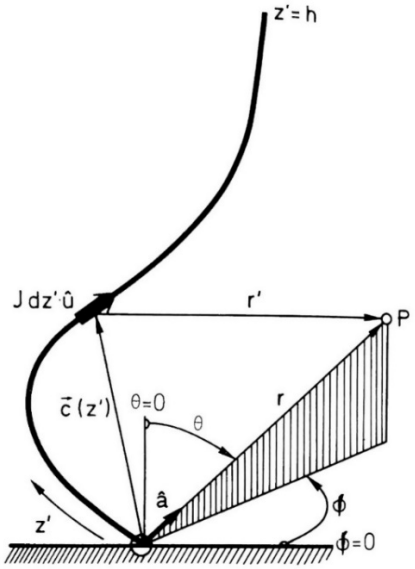

Fig 10: 3-dimensional curvilinear monopole: designations. Source: [3].

The current distribution along the antenna is sinusoidal and will not change even if the antenna shape changes, as long as the arc length $2h$ of the antenna remains constant.

The shape of the antenna of Fig. 10 can be approximated by n straight-line sections of constant length Δs.

As shown in Fig. 11, the antenna shape is given by the $2n$ angles $\alpha_1 \ldots \alpha_n$ and $\psi_1 \ldots \psi_n$ or the spatial directions of the different antenna sections as described by the unit vector $\hat{U}_1 \ldots \hat{U}_n$

For a single-wire antenna, maximum directivity is obtained with a configuration completely restricted to the E-plane.

Fig. 12 shows that the profile for maximum directivity differs from that for maximum effective height in that it has a smaller tilt and is superior in directivity by about 0.6 dB.

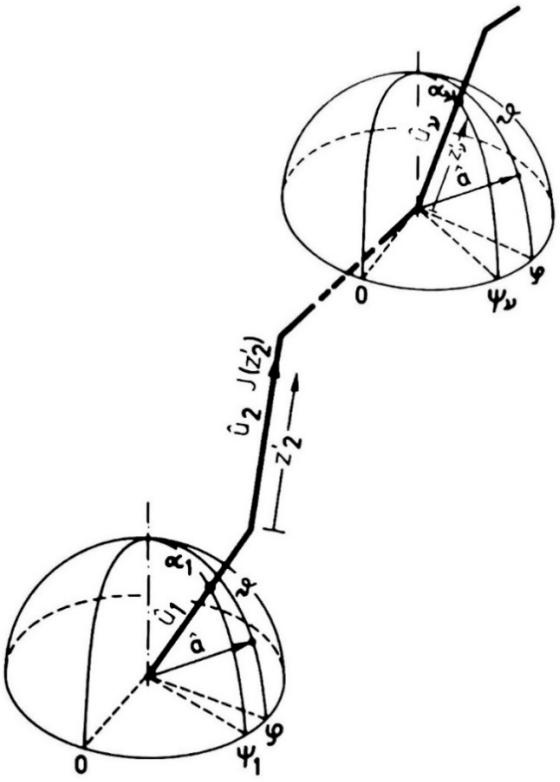

Fig 11: 3-dimensional curvilinear monopole approximated by *n* straight line sections: designations. Source: [3].

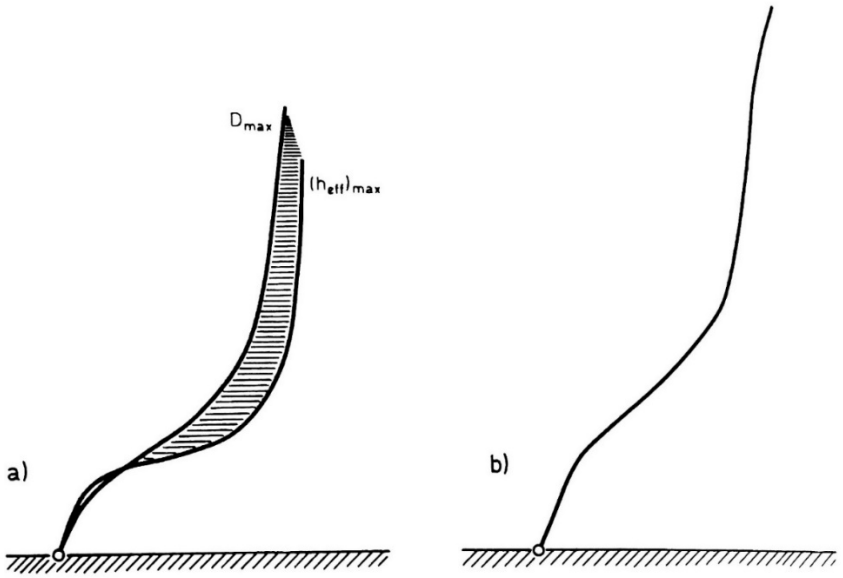

Fig 12: (a) Continuous profile for maximum directivity and maximum effective length (b) λ_0 - monopole optimized for maximum directivity. Source: [3].

One can show that a simple stick model of the monopole can also be optimized for maximum gain with 3 piecewise linear sections as shown in Figure 13. That monopole is over a perfectly electrically conducting (PEC) ground plane. The optimization varied the lengths of each section to achieve the goal of the maximum gain along the ground plane (theta = 90 degrees) as well as to achieve a second goal of a VSWR less than 1.1 into 50 ohms. The optimized sections were as follows: Length of the fed section attached to the ground plane is 0.617 wavelengths, length of the horizontal section is 0.236 wavelengths, length of the top vertical section is 0.412 wavelengths, and the radius of the wires is 0.001 wavelengths. The elevation pattern is shown in Figure 14, and the maximum gain is 10.1 dBi or about 5 dB more than for a quarter-wave vertical.

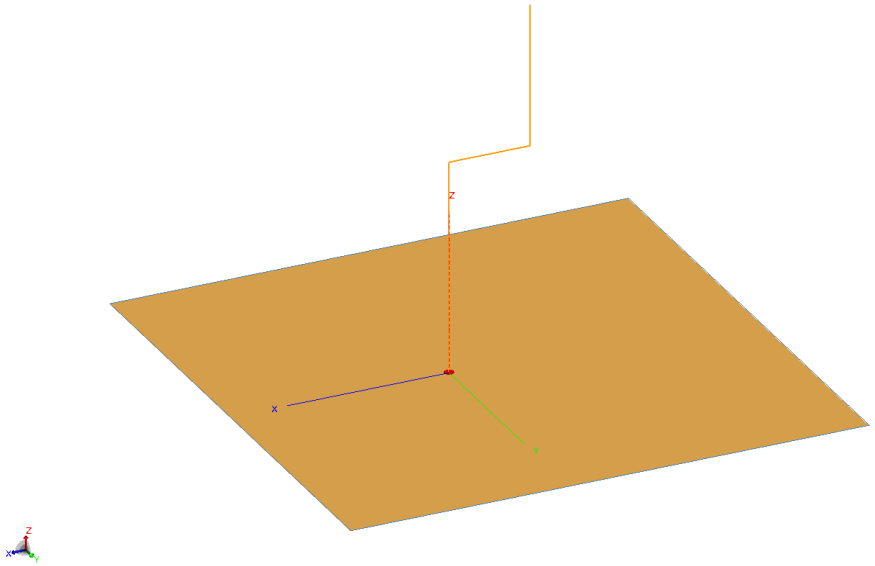

Figure 13: Altair FEKO model of piecewise linear 3 segment monopole.

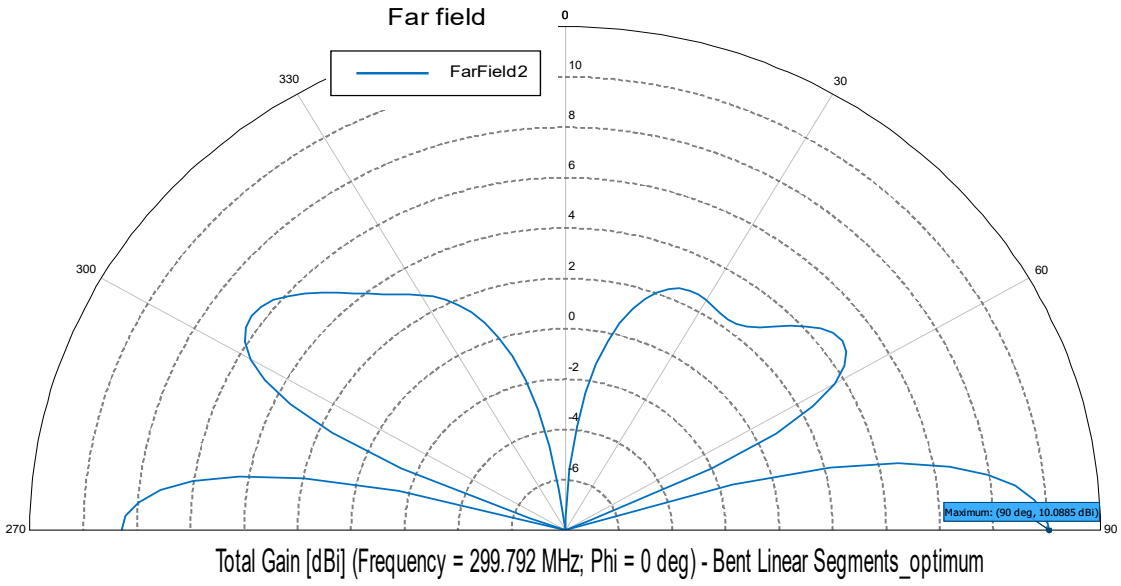

Figure 14: Elevation pattern of optimized piecewise linear 3 section monopole.

Figures 15 to 19 show modern modeling results of the curved monopole, where the results can be utilized for further optimization and impedance matching.

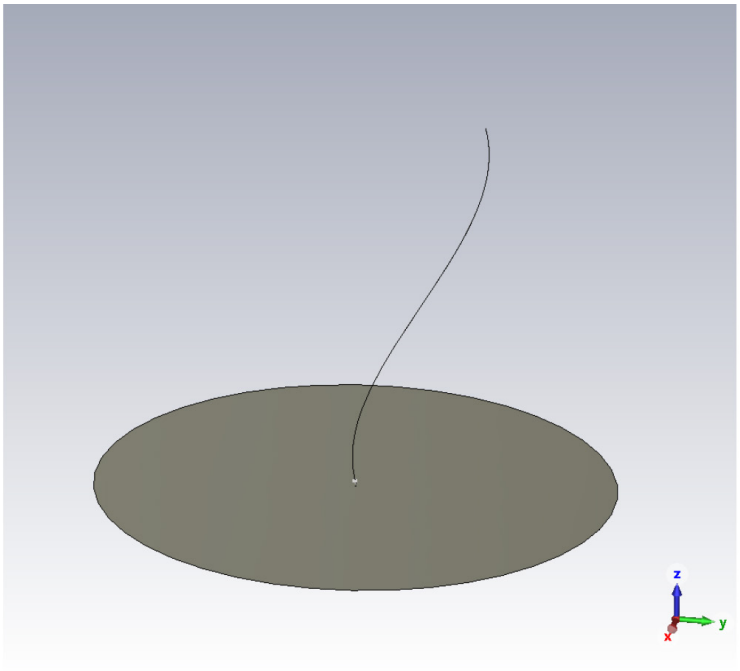

Fig. 15: CST Studio Suite model of ¾ λ antenna curvilinear antenna for simulation.

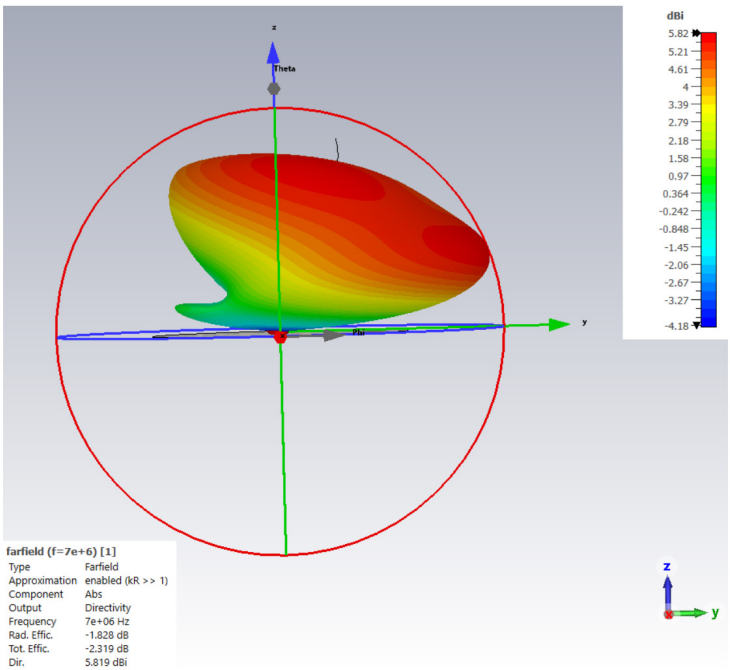

Fig. 16: CST Studio Suite radiation pattern simulation (2D).

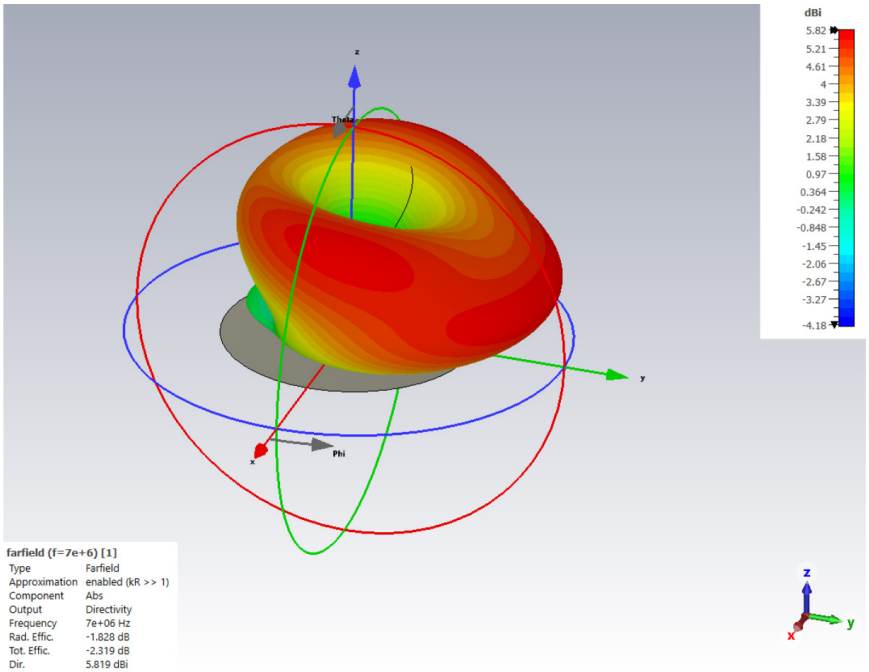

Fig. 17: CST Studio Suite radiation pattern simulation (3D).

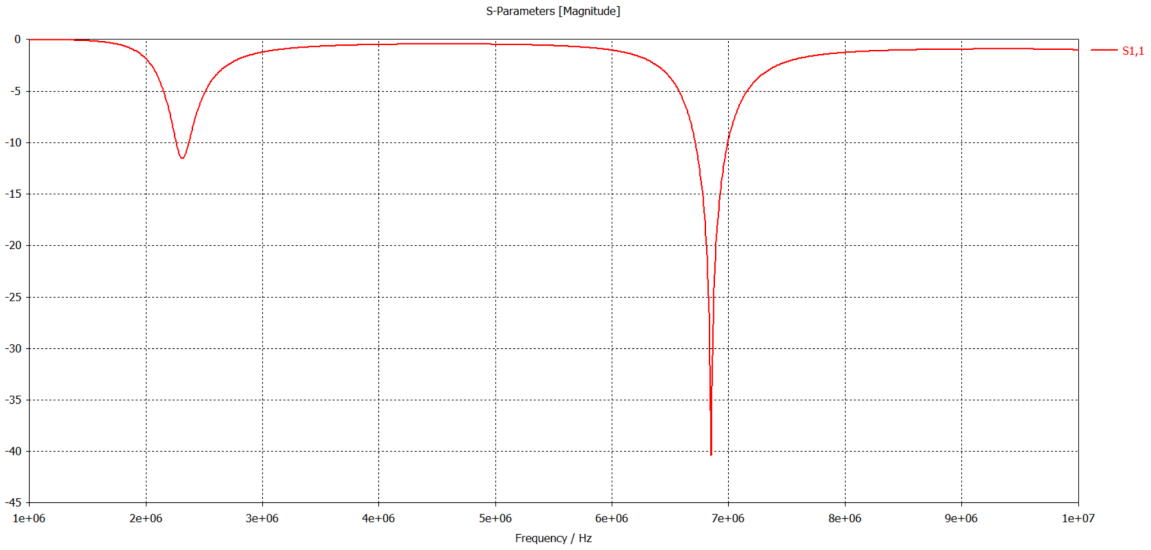

Fig. 18: Input matching simulated by CST Studio Suite.

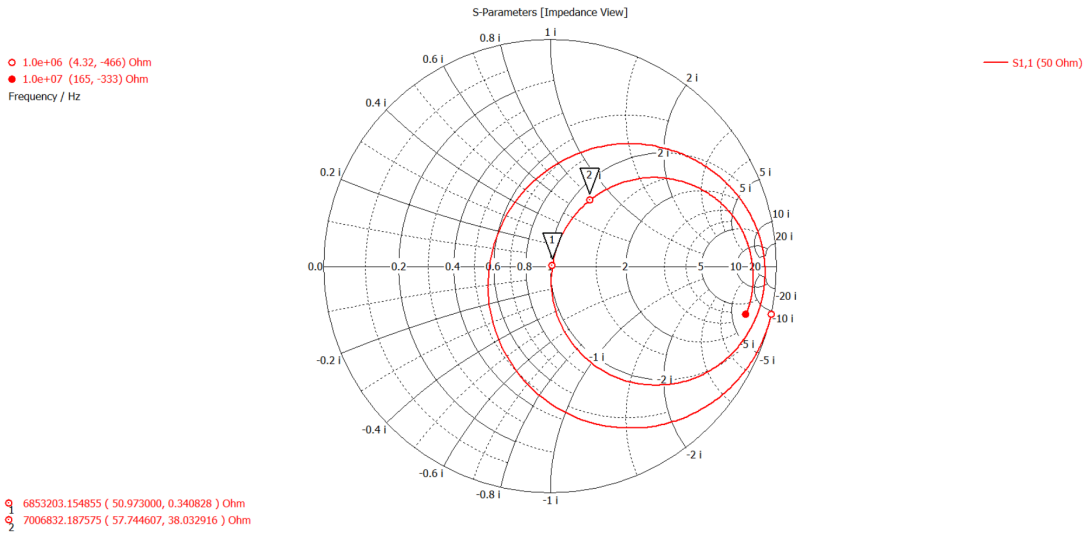

Fig. 19: CST Studio Suite simulated antenna input impedance.

Furthermore, optimization in Altair FEKO has been applied to the same 7 MHz curvilinear antenna with a height of 3/4 wavelengths over earth with a relative permittivity of 13 and a conductivity of 0.005 S/m (average ground conditions) ref [3-7]. A spline representation of the curved wire is input to the antenna software with points at each 0.15 wavelengths of height. At each point, the width dimension can be stretched plus or minus 0.5 wavelengths maximum. These are the constraints of the Genetic Optimization. There are 5 such points to give a maximum height of the antenna of 3/4 wavelengths. Curvilinear segments form the wire for the Method of Moments formulation. The antenna is fed against a conduction ground plane 0.5 wavelengths in diameter above the earth ground.

An optimization was run with maximizing the gain at a 20 degree takeoff angle above the ground while also minimizing the peak back lobe in the rear of the pattern from 0 to 90 degrees in elevation and 90 to 270 degrees in azimuth. This will find the peak back lobe in this 3D region of space and minimize it. This will give the global best front to back ratio that can be achieved for this specified region of space.

Figs. 20 to 24 show all the results from the global Genetic Optimization of the curved antenna where the optimized shape has been determined for this height of 3/4 wavelengths above the ground. The gain was 4.3 dBi which is about 4.3 dB of gain over a standard 1/4 wavelength monopole which has a gain of 0 dBi over earth ground with a good 0.5 wavelength diameter ground plane.

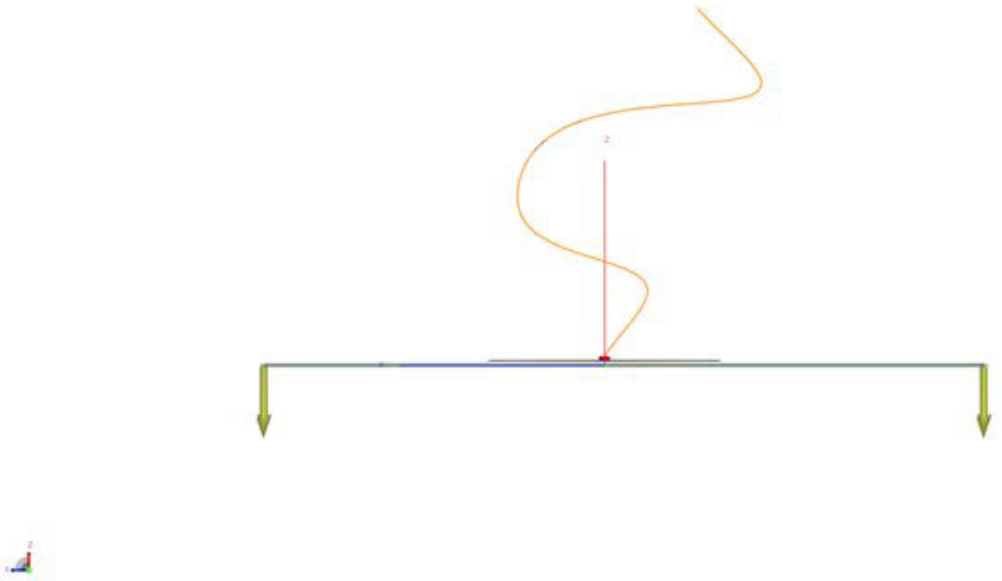

Figure 20: Altair FEKO model of optimized curved wire shape.

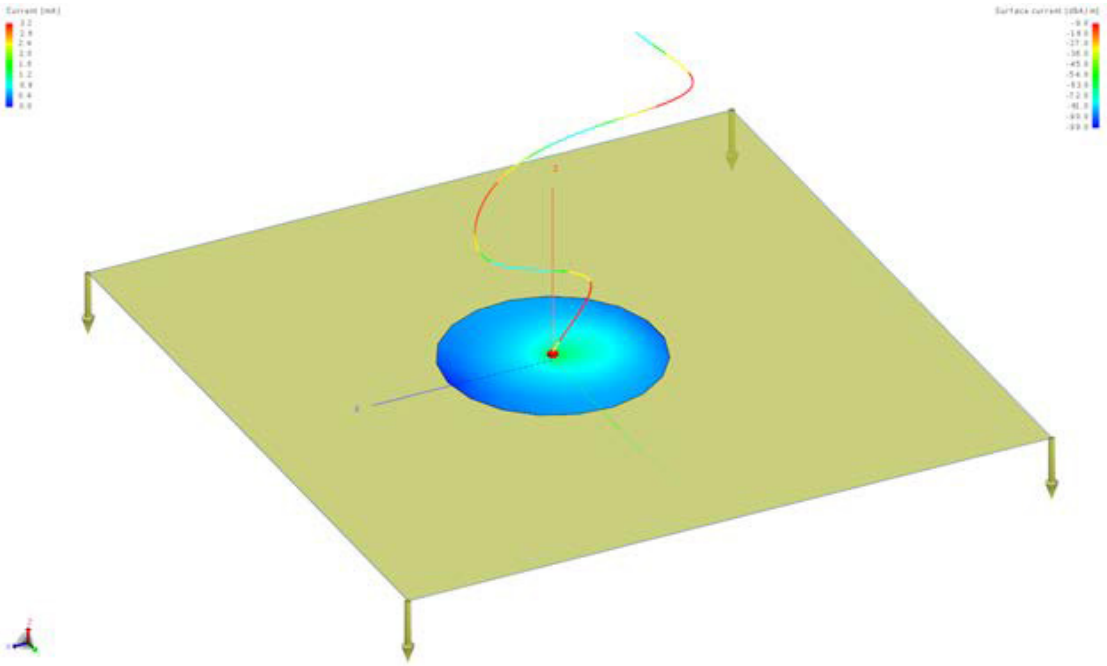

Figure 21: Current Distribution obtained by Altair FEKO.

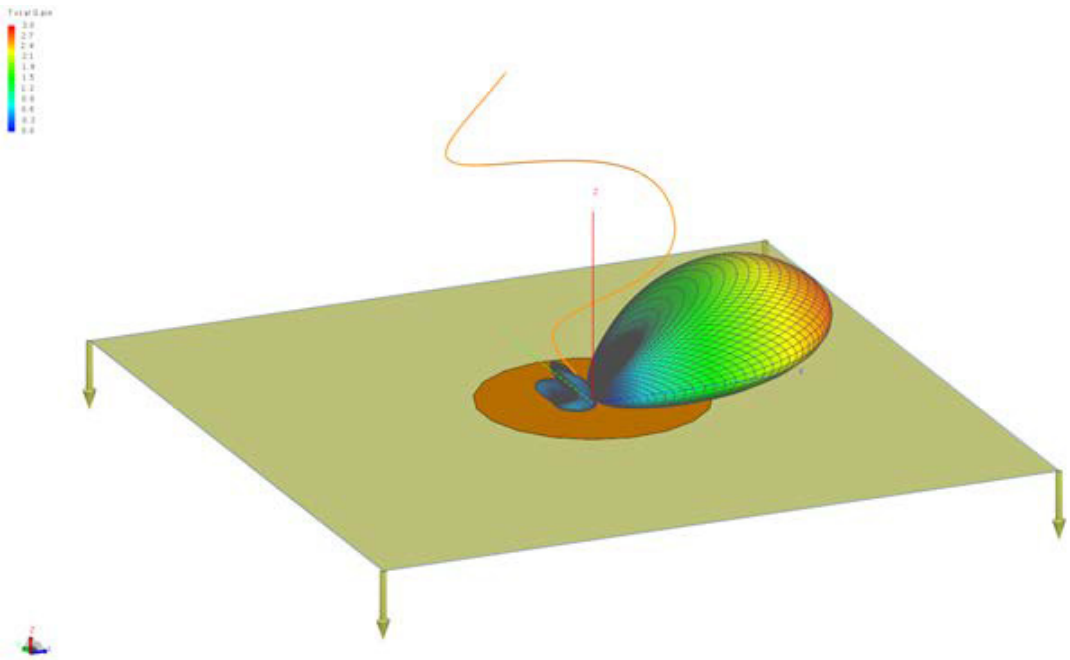

Fig. 22: 3D Pattern obtained by Altair FEKO.

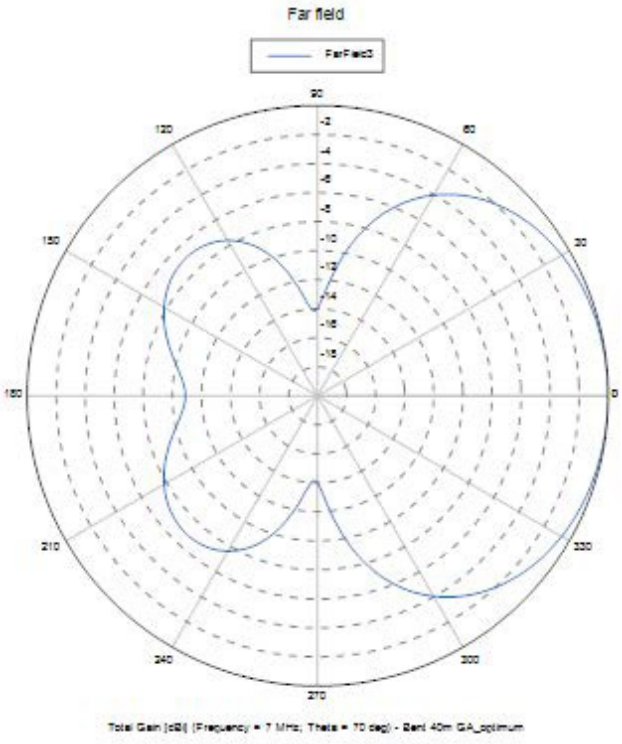

Fig. 23: Azimuth Pattern at a takeoff angle of 20 degrees.

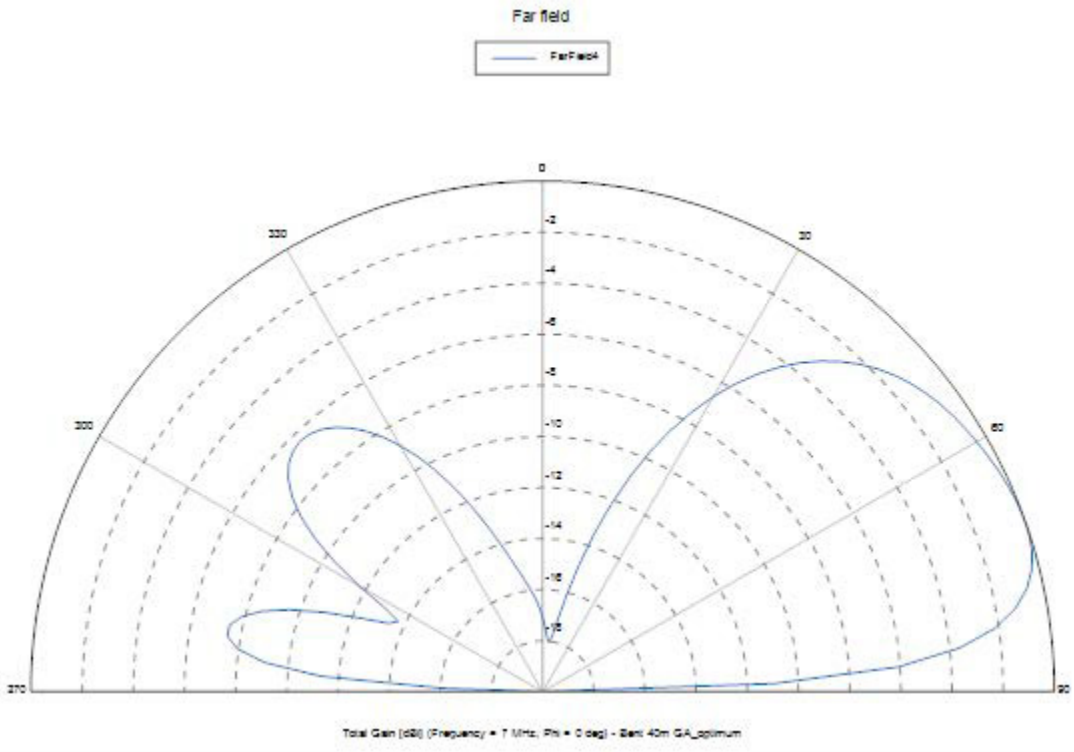

Fig. 24: Elevation Pattern.

Conclusions

This paper has shown the historical methods of computing antenna currents on wires of any arbitrary shape. Furthermore, the modern Method of Moments technique has been used with the Genetic Optimization method to obtain the optimum curved shaped for the wire monopole type of antenna to achieve the best front to back ratio for a fixed height of 3/4 wavelengths.

This is a very simple method to achieve such performance of just one simple wire compared to more complex arrays of multiple antennas necessary to achieve similar performance.

References

[1] Schaefer, CL.: Einführung in die theoretische Physik (Introduction into Theoretical Physics), Bd. 3/1 S. 331, Berlin: W.de Gruyter 1932.

[2] Burstyn. W.: Die Strahlung und Richtwirkung einiger Luftdrahtformen im freien Raum (Radiation and Direction of Different styles of Open Wire Antennas), Jb. drahtl. Telegr. Bd. 13 (1918) S. 362].

[3] F. M. Landstorfer, and R. R. Sacher, “Optimisation of Wire Antennas”, Research Studies Press Ltd., 1985, ISBN 0863800254

[4] Hans Ludwig Hartnagel, Rudiger Quay, Ulrich L. Rohde, Matthias Rudolph, “Fundamentals of RF and Microwave Techniques and Technologies”, Ch.6.

[5] G. II. Brown and R. King, "High Frequency Models is Antenna Investigations, "Proc. IRE, 22,457-480, April1934.

[6] Kazimierz “Kai” Siwiak, (KE4PT), “Q and the Energy Around Antennas”, QST Feb 2013, pp-37

[7] FEKO, Altair Engineering Inc., 2022

[8] Siwiak K., Rohde U. L., “Tuning electrically short antennas for field operation”, Microwave Journal, May2019

[9] Kraus, John Daniel, “Antennas”, second edition, McGraw Hill, 1988, ISBN0-07-035422-7

[10] S. A. Schelkunoff, Applied Mathematics for Engineers and Scientists, Van Nostrand, New York, 1948. p377)

Further Reading

- J. K. Breakall, "New Ideas from Computer Models," Antenna Forum, Dayton Hamvention, Dayton, Ohio, 1993.
- J. K. Breakall, "Computer Modeling of Antennas Using NEC and MININEC," 32nd Midwest Symposium on Circuits and Systems, Champaign, IL, 1989.
- J. M. Stamm, M. W. Fenton, and J. K. Breakall, “Comparison and Results for Models of a Thick Bent-Wire Dipole Using NEC4 and WIPL,” Applied Computational Electromagnetics Symposium, Monterey, CA, March, 1999.
- J. K. Breakall, J. S. Young, R. J. Bauerle, A. I. McDowell and T. A. Erdley, "Numerical Electromagnetics Code Optimization Design Software (NECOPT)," 10th Annual Review of Progress in Applied Computational Electromagnetics, Naval Postgraduate School, Monterey, CA, 1994.
- J. K. Breakall, J. S. Young and G. Hagn, "Measurement and Modeling of HF Monopoles and Dipoles in Irregular Terrain," DARPA, AFCEA, and IEEE Tactical Communications Conference Proceedings, 1992.

- J. K. Breakall, "Computer Analysis of Vertical Antenna Systems Over Earth," Antenna Forum, Dayton, Ohio, 1984.
- J. K. Breakall, "Computer Antenna Modeling," Antenna Forum, Dayton Hamvention, Dayton, Ohio, 1983.
- J. K. Breakall, G. J. Burke, and E. K. Miller, "The Numerical Electromagnetics Code (NEC)," EMC Symposium and Exhibition, Zurich, Switzerland, 1985.
- R. J. Bauerle and J. K. Breakall. Comparison of Input Impedance of Monopole Antennas Obtained by NEC, MININEC, and Measurements. Applied Computational Electromagnetics Society Journal 10(2): July, 1995, 75-85.
- J. K. Breakall, D. H. Werner and R. J. Lunnen. Antenna Modeling and Characterization of a VLF Airborne Dual Trailing Wire Antenna System. The Applied Computational Electromagnetics Society Journal 9(1): March, 1994, 18-31.
- Cheng, D. K. and Liang, C. H., "Shaped Wire Antennas with Maximum Directivity," Electronics Letters, 18, 19, September 16, 1982, pp. 816-818.
- Altshuler, E. E. and Linden, D. S., "Wire-Antenna Design Using Genetic Algorithms," IEEE Antennas and Propagation Magazine, 39, 2, April 1997, p. 33-43.
- Rabelo. R. and Terada, M., “Analysis and Optimization of Wire Antennas over the Internet,” IEEE Antennas and Propagation Magazine, Vol. 521, No. 1, February2010.